ENERGY AND EXERGY ASSESSMENTS OF A SINGLE FLASH GEOTHERMAL AND ORC SYSTEM WITH PACKED BED STORAGE USING OLIVE POMACE

by

Deniz YILDIRIM YALCINKAYA[a*], Arif HEPBASLI[b], and Huseyin GUNERHAN[c]

[a] Graduate School of Natural and Applied Sciences, Department of Mechanical Engineering, Ege University, Izmir, Turkey
[b] Faculty of Engineering, Department of Energy Systems Engineering, Yasar University, Izmir, Turkey
[c] Faculty of Sciences, Department of Mechanical Engineering, Ege University, Izmir, Turkey

Original scientific paper
https://doi.org/10.2298/TSC2504229Y

This study presents a detailed analysis of a packed bed thermal energy storage system, supported by a critical review of similar configurations in the literature. The research emphasizes the impact of working fluids on overall system performance. Key parameters including thermal storage capacity, heat transfer mechanisms, pressure drop, air-flow velocity, biomass feed rate, and heat transfer fluid temperature are assessed for their roles in determining system behavior. The main objective is to develop an innovative system that integrates an ORC with a single flash geothermal unit. Thermodynamic assessments, covering both energy and exergy analyses, were performed using MATLAB in conjunction with the CoolProp library to ensure precise thermophysical property data. Departing from conventional geothermal set-ups, this study introduces a novel ORC-SFGEO integration. While R245fa remains a benchmark working fluid, the study also evaluates low global warming potential alternatives including R1233zd(E), R1234ze(Z), R1234ze(E), and R1234yf commonly used in heat pumps to enhance thermodynamic and environmental performance. Results show that the integrated system yields a 40% performance increase compared to similar systems in the literature. The energy and exergy efficiencies of the base system, without a heat pump, are 24.26% and 7.51%, respectively. When the HPS is integrated, exergy efficiency improves by 55.5%, addressing fluctuations in solar input.

Key words: *packed bed thermal energy storage, ORC, waste heat recovery, single flash geothermal energy cycle, exergy analysis*

Introduction

With the growing global energy demand, integrating thermal energy storage (TES) with RES such as solar, wind, geothermal, and biomass has become critical for reducing dependence on fossil fuels and ensuring uninterrupted energy supply. Forecasts indicate that TES technologies will comprise nearly 60% of the total heat storage capacity between 2030 and 2050. Furthermore, compared to hydrogen storage and lithium-ion batteries, TES is considerably more cost-effective [1, 2].

Among TES technologies, packed bed thermal energy storage (PTES) systems have received considerable attention in both experimental and theoretical research. These systems

* Corresponding author, e-mail: denizyildirim198748@gmail.com

typically consist of a tank filled with suitable packing materials and a heat transfer fluid (HTF), which may be either a liquid or gas. Liquid HTF allow operation at lower Reynolds numbers, minimizing pumping power, while gas HTF, like air, benefit from low viscosity and high temperature operation [3].

Jan's research applied a multi-objective optimization strategy to air operated, thermocline-layered PTES systems to enhance exergy efficiency and reduce material costs. The study found that a narrow top-truncated cone design offered the highest exergy efficiency, and the method used reduced computation time by up to 99% [4]. In a related 2019 study, Singh *et al*. [5] used a modified 1-D two-phase Schumann model to simulate a 175000 m³ conical packed bed. The system exhibited over 98% energy and exergy efficiency under optimal parameters like 3 cm rock diameter and 0.6 m insulation thickness. Hassan *et al*. [6] reported that the smallest cone cross-section in TES design resulted in the highest exergy performance, recovering 33% of stored energy with only 4.22 kW fan power required.

Pressure drop, a critical factor in PTES efficiency, is influenced by packing material porosity and other parameters like particle diameter, air-flow velocity, and tank geometry [3, 7, 8]. Trevisan *et al*. [9] found that using larger gravel and medium particles offered economic benefits while enhancing performance. Gautam and Saini [10] study noted that while higher air-flow rates increase energy consumption, they are also shaped by the tank's *L*/*D* aspect ratio, which affects the overall flow and heat transfer behavior [11]. To further optimize PTES performance, system parameters such as pressure drop, outlet temperature, insulation thickness, fan power, thermal capacity, Reynolds, Nusselt, and Biot numbers, and material costs must be simultaneously tuned. For example, Charmala developed empirical correlations to estimate Nusselt numbers and heat transfer coefficients for different PTES packing geometries and materials, assisting designers in system development [2, 12-17].

Research also highlights various integration methods to boost PTES performance. Christian's density based optimization with rock and sand packing improved TES system performance by 46% [18]. Cardenas *et al*. [19] showed that an aspect ratio of 0.6 mm and 4 mm particles maximized exergy efficiency (98.24%) while enabling drying during sunless periods. Atalay and Cankurtaran [20] reported that a solar air collector integrated PTES system had a 6.82-year energy pay-back period, cutting CO_2 emissions by 99.60 tons. Lamrani and Draoui [21] TRNSYS-based Moroccan climate study showed that PTES-enhanced solar wood drying could reduce drying time by 15% and pay-back time by 33%.

Waste biomass, such as olive pomace, can be dried in PTES systems and combusted in ORC systems for sustainable energy recovery. The ORC working fluid choice particularly low GWP alternatives like R1233zd(E), R1224yd(Z), and R1234ze(Z) affects system performance, emissions, and material compatibility [22, 23]. Despite slight efficiency tradeoffs, they offer substantial environmental benefits compared to traditional fluids like R245fa.

Finally, literature lacks studies integrating ORC-SFGEO with PTES, though they promise low cost, sustainable power generation [24-26]. Turkey's olive rich regions offer potential for using dried pomace in PTES supported ORC systems, enabling local energy production, better waste management, and improved drying efficiency up to 18% [27, 28]. This study proposes an innovative, integrated approach to enhance sustainable energy recovery and regional development.

Material and method

In the system considered, a hybrid waste energy conversion system has been developed by integrating olive pomace biomass, dried through an air solar collector supported PTES

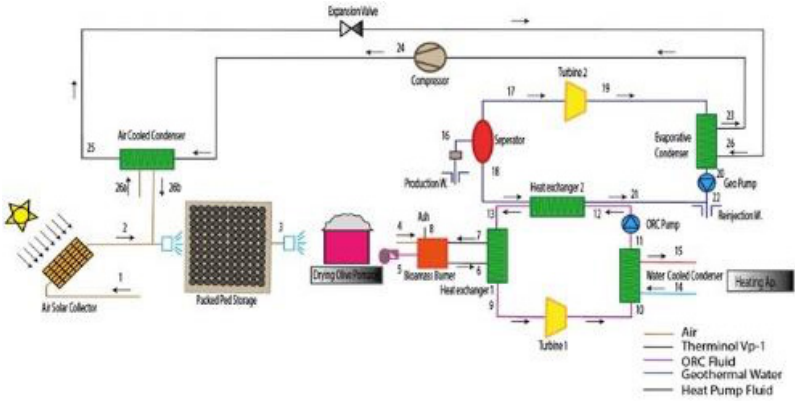

Figure 1. Schematic Model of PTES

system, with an ORC system and a single flash geothermal energy cycle. Additionally, a heat pump system has been integrated as an alternative to packed bed storage due to the intermittent nature of solar energy. This hybrid energy system is an innovative approach that combines solar, biomass, and geothermal energy to provide both electricity generation and heating.

The system's operating principle is illustrated in fig. 1. Solar energy is harvested via supported air collectors and stored in a packed bed heat storage unit, later used for drying

Table 1. Energy and exergy balance equations of PTES components

Component	Exergy balance
Solar collector	$\dot{E}x_{\text{solarin}} = \dot{E}x_{\text{u}} + \dot{E}x_{\text{destsolar}} + \dot{E}x_{\text{losssolar}}$
Packed bed storage	$\dot{E}x_{\text{u}} + 2\times\dot{W}_{\text{fan}} = \dot{E}x_{\text{packed,a}} + \dot{E}x_{\text{destpacked}} + \dot{E}x_{\text{packed,loss}}$
Geothermal separator	$\dot{E}x_{\text{sep16}} = \dot{E}x_{\text{sep17}} + \dot{E}x_{\text{sep18}} + \dot{E}x_{\text{destsep}} + \dot{E}x_{\text{losssep}}$
Biomass burner	$\dot{E}x_{\text{burnerbio}} + \dot{E}x_{\text{terminol7}} = \dot{E}x_{\text{pomash}} + \dot{E}x_{\text{terminol6}} + \dot{E}x_{\text{destburner}} + \dot{E}x_{\text{lossburner}}$
Heat exchanger 1	$\dot{E}x_{9} + \dot{E}x_{\text{terminol6}} = \dot{E}x_{13} + \dot{E}x_{\text{terminol7}} + \dot{E}x_{\text{destheatexc1}} + \dot{E}x_{\text{lossheatexc1}}$
Heat exchanger 2	$\dot{E}x_{12} + \dot{E}x_{18} = \dot{E}x_{13} + \dot{E}x_{21} + \dot{E}x_{\text{destheatexc2}} + \dot{E}x_{\text{lossheatexc2}}$
Orc turbine	$\dot{E}x_{9} = \dot{E}x_{10\text{a}} + \dot{W}_{\text{turb1}} + \dot{E}x_{\text{destturb1}} + \dot{E}x_{\text{lossturb1}}$
Geothermal turbine	$\dot{E}x_{17} = \dot{E}x_{19\text{a}} + \dot{W}_{\text{turb2}} + \dot{E}x_{\text{destturb2}} + \dot{E}x_{\text{lossturb2}}$
ORC condenser	$\dot{E}x_{10\text{a}} + \dot{E}x_{14} = \dot{E}x_{11} + \dot{E}x_{15} + \dot{E}x_{\text{destbiocond}} + \dot{E}x_{\text{lossbiocond}}$
ORC pump	$\dot{E}x_{12} + \dot{W}_{\text{pumpbio}} = \dot{E}x_{11} + \dot{E}x_{\text{destbiopump}} + \dot{E}x_{\text{lossbiopump}}$
Geothermal pump	$\dot{E}x_{22} + \dot{W}_{\text{pumpgeo}} = \dot{E}x_{20} + \dot{E}x_{\text{destgeopump}} + \dot{E}x_{\text{lossgeopump}}$
Evaporative condenser	$\dot{E}x_{19\text{a}} + \dot{E}x_{27} = \dot{E}x_{20} + \dot{E}x_{23} + \dot{E}x_{\text{destcondsog}} + \dot{E}x_{\text{losscondsog}}$
Compressor	$\dot{E}x_{23\text{sog}} - \dot{E}x_{24\text{sog}} + \dot{W}_{\text{kompsog}} = \dot{E}x_{\text{destkompsog}} + \dot{E}x_{\text{losskompsog}}$
Air cooled condenser	$\dot{E}x_{27\text{sog}} + \dot{E}x_{19} = \dot{E}x_{23\text{sog}} + \dot{E}x_{20} + \dot{E}x_{\text{destcondsog}} + \dot{E}x_{\text{losscondsog}}$
Reducing valve	$\dot{E}x_{25\text{sog}} - \dot{E}x_{27\text{sog}} = \dot{E}x_{\text{destgensog}} + \dot{E}x_{\text{lossgensog}}$

olive pomace biomass. The analytical model incorporates governing equations for the air solar collector, packed bed, and biomass combustion chamber components [11, 29]. Following the approach of Mumma and Marvin, temperature differentials are central to modelling the packed bed's thermal profile. The 2 m gravel bed is discretized into 20 sections, each spaced 10 cm apart. Fan power requirements are derived from pressure drop estimations. The biomass combustion chamber equations are sourced from established models [7, 26, 27, 30]. Table 1 summarizes energy and exergy balance equations for each PTES component, critical for evaluating thermodynamic behavior and system efficiency.

Energy and exergy analysis

In the general system analysis, the system boundary is defined to exclude the heat pump, while including all other system components. The thermodynamic assumptions considered for the PTES system are: the system operates under steady-state conditions, changes in potential and kinetic energy are neglected, friction losses are neglected, the ambient pressure and temperature are taken as P_0 = 101.325 kPa and T_0 = 25 °C. The key parameters and design values critical for determining the performance of the analyzed TES and conversion system are summarized in the table below, tab. 2 [7, 26, 31-35].

The exergy analysis table, tab. 3 presents the thermodynamic performance and exergy losses of each component of the system in detail. This analysis is crucial for identifying the main sources of inefficiency within the system and pinpointing optimization opportunities. Sustainability analysis in energy systems plays a crucial role in assessing the environmental benefits or adverse impacts of these systems, particularly in terms of their environmental contributions and waste generation [36].

Results and discussion

In the system performance analysis, MATLAB was employed for numerical modelling, while thermophysical properties of the working fluids were determined using the COOLPROP library. Reported second law efficiency values range from 4.7%-93%, indicating varying degrees of exergy losses. Enhancing these values is critical for improving the sustainability and economic feasibility of thermal energy systems. Recent high efficiencies, such as those reported by Alice and Paul, reflect notable advancements in the field [37-39]. Dejene's study investigated a parabolic solar collector coupled with a gravel packed bed cooker for tropical regions, achieving 30% cooking efficiency and 66.7% thermal storage efficiency under high solar irradiance, while dropping to 22.08% under low irradiance [40]. Figure 2 illustrates that 60% of exergy destruction occurs in the biomass combustion chamber, 22% in heat Exchanger 1 and the ORC condenser, and 18% in remaining components.

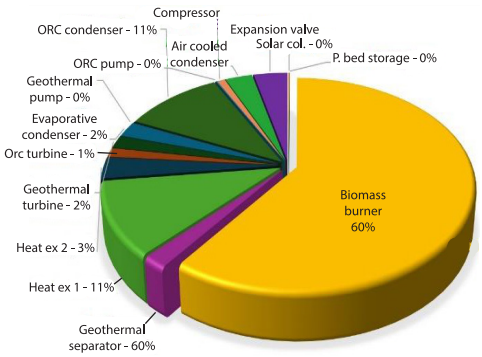

Figure 2. The exergy destruction rates of PTES components

As shown in fig. 3(a), minimizing the pressure drop in the packed bed storage system is crucial due to its significant impact on the system's exergy efficiency. A reduced pressure drop lowers the required fan power, thereby enhancing the overall performance of the system. In fact, as the pressure drop, D_p decreases, the fan power consumption, W_{fan} also decreases approximately linearly.

Table 2. Operating tables of PTES

Parameters	Units	Values
Solar radiation, I	[Wm^{-2}]	779.03
Solar radiation temperature, T_{Sun}	[K]	6000
Solar collector area, A_{scol}	[m^2]	6
Air specific heat capacity, $C_{p,a}$	[$kJkg^{-1}K^{-1}$]	1008
Specific heat capacity of moist air, $C_{p,va}$	[$kJkg^{-1}K^{-1}$]	0.72
Ambient temperature, T_{amb}	[K]	298.15
Solar collector outlet temperature, T_{aout}	[K]	348.15
Solar collector inlet temperature, T_{ain}	[K]	298.15
F_R ($\bar{\alpha}$ α)	[–]	0.60
F_R U_L	[–]	3
Packed bed inlet temperature, $T_{aipacked}$	[K]	348.15
Packed bed sections, A_{packed}	[m^2]	4
Air inlet velocity into the packed bed, V_a	[ms^{-1}]	0.20
Air density, q_a	[kgm^{-3}]	1.10
Inlet temperature from collector to packed bed, T_{ai}	[K]	348.15
Initial temperature of packed bed, T_{bi}	[K]	298.15
Charging time, t	[second]	28800
Void fraction, ε	[–]	0.30
Sphericity of storage material, φ	[–]	0.80
Pebble stone density, q_s	[kgm^{-3}]	1920
Pebble stone specific heat capacity, $C_{p,s}$	[$Jkg^{-1}K^{-1}$]	835
Packed bed volume, V_b	[m^3]	8
Pebble stone diameter, D_e	[m]	0.05
Pebble stone thermal conductivity, K_s	[$Wm^{-1}K^{-1}$]	2
Bed length, L	[m]	2
Number of bed materials, N	[–]	20
Time range, Δt	[second]	900
R_a	[$kJkg^{-1}K^{-1}$]	0.2870
Isentropic Turbine 1 efficiency, μ_{st1}	[–]	0.85
Isentropic Turbine 2 efficiency, μ_{st2}	[–]	0.83
T_{Hsog}	K	313.15
Pump motor isentropic efficiency, μ_{pump}	[–]	0.95
Isentropic compressor efficiency, μ_{sc}	[–]	0.85
Water specific heat capacity, $C_{p,geo}$	[$kJkg^{-1}K^{-1}$]	4.18
Olive pomace specific heat capacity, $C_{p,pom}$	[$kJkg^{-1}K^{-1}$]	1.63
Therminol specific heat capacity, $C_{p,therminol}$	[$kJkg^{-1}K^{-1}$]	1.53
The R-245fa specific heat capacity ($C_{p,r245fa}$)	[$kJkg^{-1}K^{-1}$]	1.36
The R-1234yf specific heat capacity ($C_{p,r1234yf}$)	[$kJkg^{-1}K^{-1}$]	1.28
Olive pomace moisture content, w_b [%]	[–]	14.60
Water voparization enthalpy in olive pomace, $h_{fgolivepom}$	[$kJkg^{-1}$]	2500
Air excess coefficient, λ	[–]	0.20
C [%]	[–]	52.90
H [%]	[–]	8.94
N [%]	[–]	2.54
O [%]	[–]	31.82
S [%]	[–]	0
Ash [%]	[–]	3.80

Table 3. The PTES energy, exergy and exergy destruction values

Components	Exergy fuel flow [kW]	Exergy product flow [kW]	Exergy destruction [kW]	Exergy efficiency
Solar collector	4.36	0.20	4.14	0.04
Packed bed storage	0.22	0.15	0.07	0.63
Biomass burner	2328.30	741.71	1562.90	0.30
Heat exchanger 1	741.71	449.29	291.52	0.60
ORC turbine	332.25	288.02	36.45	0.84
ORC condenser	326.07	50.14	275.79	0.15
ORC pump	33.37	30.78	2.59	0.92
Heat exchanger 2	260.26	175.66	84.38	0.67
Geothermal seperator	858.10	806.02	50.77	0.93
Geothermal turbine	314.01	263.27	50.43	0.83
Evaporative condenser	99.83	38.34	61.47	0.38
Geothermal pump	0.20	0.01	0.18	0.94
Compressor	180.58	153.49	21.74	0.84
Air cooled condenser	102.50	26.04	76.45	0.25
Expansion valve	545.64	450.98	94.64	0.82
Geothermal flash overall				0.05
ORC overall				0.36
Heat pump overall				0.14
General overall				0.07

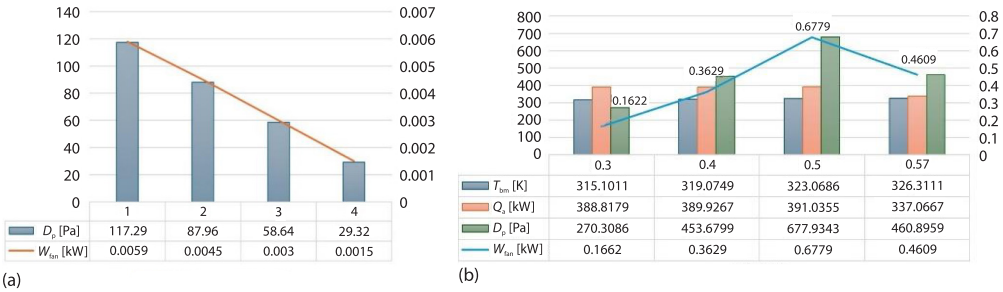

Figure 3. (a) The effect of pressure drop on fan power consumption and (b) effect of void fraction on packed bed T_{bm}, energy, and exergy efficiency

As shown in fig. 3(b), critical parameters such as void fraction, pressure drop, fan power capacity, T_{bm}, and exergy efficiency significantly impact the performance of the packed bed storage system. In this study, a void fraction value of 0.3 was used to achieve the minimum pressure drop, optimizing system performance. However, this value can still be further optimized, indicating potential for additional improvement. Table 4 compares packed bed heat exchanger efficiencies from Turkakar [41] and the present PTES model. At $T_{amb} = 15$ °C, Turkakar reported 46.42%, while this study achieved 65.57% (relative error: 0.41%). At 20 °C, efficiencies were 61.9% and 64.82% (error: 0.04%). At 25 °C, 63.84% (current) *vs.*

77.38% (Turkakar), with a 0.17% error, all below 2%. Atalay [7] experimentally studied a solar dryer with packed bed thermal storage, reporting orange slice moisture reduction from 93.5%-10.28%, and exergy efficiency from 50.18%-66.58%. As shown in fig. 4(a), the energy and exergy analysis of packed bed results obtained are consistent with the findings of [7, 41].

Table 4. The PTES model verification study

Conditions	[41] Packed bed exchanger efficiencies [%]	[7] Packed bed exchanger efficiencies [%]	Relative error [%]
T_{amb} = 15 0C	46.42	65.57	0.41
T_{amb} = 20 0C	61.9	64.82	0.04
T_{amb} = 25 0C	77.38	63.84	0.17

Turkakar [41] emphasized that air-flow above 0.1 m/s minimizes fan power and enhances tank performance. This study uses 0.2 m/s inlet air velocity for optimal exergy efficiency. As illustrated in fig. 4(b), increasing the *mterminol* flow rate from 2.06-10.33 kg/s leads to a marked reduction in overall energy efficiency (*en eff. overall*) from 29.06%-22.07% and exergy efficiency (*ex eff. overall*) from 9.84%-6.57%. Simultaneously, the biomass input *mpom* increases from 0.01-0.05 kg/s, indicating an inverse relationship with efficiencies due to rising thermodynamic losses. Colantoni *et al.* [26] reported electrical efficiencies of 12.7%-19.4% for a pomace-fueled ORC system using an LHV of 23.75 MJ/kg, while the current study uses 27.41 MJ/kg. Mellalou *et al.* [27] achieved 36.91% exergy efficiency, compared to 63% here. Table 5 shows that R1233zd(E) provides the highest turbine output (162 kW at 100 °C) among the fluids analyzed, emphasizing the importance of working fluid choice in optimizing ORC performance.

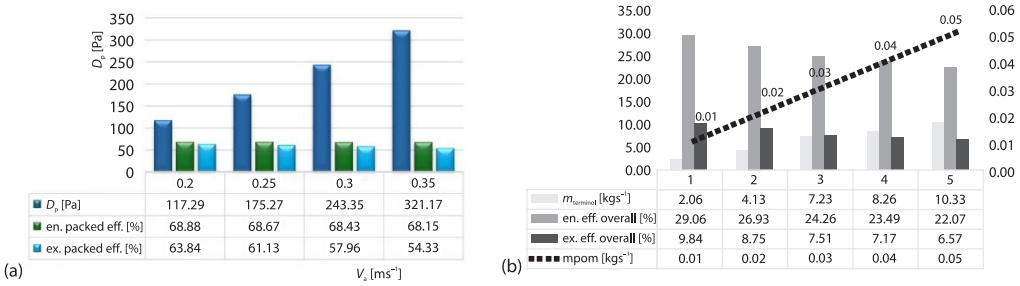

Figure 4. (a) The effect of flow velocity on pressure drop and (b) effect of olive pomace flow rate on exergy efficiency

Table 5. Comparison of turbine work rates for ORC fluids based on turbine inlet temperature

ORC turbine inlet teperature [°C]	WR245fa [kW)]	W R1233zd(E) [kW]	W R1234ze(Z) [kW)]	W R1234ze(E) [kW]
70	3.10	3.33	2.20	2.43
80	55.26	59.42	39.25	43.41
90	104.48	112.34	74.22	82.09
100	150.66	162	107.02	118.37

Conclusions

This study assessed a sustainable hybrid energy system for integrating, converting, and storing multiple energy sources. In the PTES system, increasing olive pomace flow rate reduced overall energy efficiency from 29.06%-22.07% and exergy efficiency from 9.84%-6.57%, indicating higher irreversibilities.

Maximum exergy efficiency was achieved at an air velocity of 0.2 m/s. The biomass combustor exhibited the highest exergy destruction (1562.90 kW), followed by heat Exchanger 1 (291.52 kW) and the ORC condenser (275.79 kW). The geothermal separator (93%), ORC pump (92%), and geothermal pump (94%) had the highest efficiencies, while the solar collector (4%), ORC condenser (15%), air-cooled condenser (25%), and evaporative condenser (38%) showed the lowest.

Overall exergy efficiencies were 5% (geothermal), 36% (ORC), and 14% (heat pump). Integration of the heat pump improved packed bed efficiency by 55.5%, reaching 98%. Literature reports efficiencies from 4.7%, Dhivagar *et al.* [37], to 93%, Tosatto *et al.* [38]. Fan power use was minimized at air velocities >0.1 m/s, with 0.2 m/s selected for high performance (error <2%). R1233zd(E) delivered the highest ORC turbine work (162 kW at 100 °C), while R1234ze(Z) was lowest. Overall, the system provides an efficient, scalable model for sustainable energy use, especially in agricultural waste rich regions.

References

[1] [Maruf, M. N. I., *et al*., Classification, Potential Role, and Modelling of Power-to-Heat and Thermal Energy Storage in Energy Systems: A Review, *Sustainable Energy Technologies and Assessments*, *53*, (2022), Part B, 102553
[2] Gautam, A., Saini, R. P., Experimental Investigation of Heat Transfer and Fluid-Flow Behavior of Packed Bed Solar Thermal Energy Storage System Having Spheres As Packing Element with Pores, *Solar Energy*, *204* (2020), July, pp. 530-541
[3] Kocak, B., *et al*., Review on Sensible Thermal Energy Storage for Industrial Solar Applications and Sustainability Aspects, *Solar Energy*, *209* (2020), Oct., pp. 135-169
[4] Marti, J., *et al*., Constrained Multi-Objective Optimization of Thermocline Packed-Bed Thermal-Energy Storage, *Applied Energy*, *216* (2018), Apr., pp. 694-708
[5] Singh, S., *et al*., Investigation on transient Performance of a Large-Scale Packed-Bed Thermal Energy *Storage, Applied Energy*, *239* (2019), Apr., pp. 1114-1129
[6] Hassan, A., *et al*., Transient Analysis and Techno-Economic Assessment of Thermal Energy Storage Integrated with Solar Air Heater for Energy Management in Drying, *Solar Energy*, *264* (2023), 112043
[7] Atalay, H., Performance Analysis of a Solar Dryer Integrated With the Packed Bed Thermal Energy Storage (TES) System, *Energy*, *172* (2019), Apr., pp. 1037-1052
[8] Singh, H., *et al.*, A review on packed bed solar energy storage systems, Renewable and Sustainable Energy Reviews, *14* (2010), 3, pp. 1059-1069
[9] Trevisan, S., *et al*., Packed Bed Thermal Energy Storage: A Novel Design Methodology Including Quasi-Dynamic Boundary Conditions and Techno-Economic Optimization, *Journal of Energy Storage*, *36* (2021), 102441
[10] Gautam, A., Saini, R. P., Thermal and Hydraulic Characteristics of Packed Bed Solar Energy Storage System Having Spheres As Packing Element With Pores, *Journal of Energy Storage*, *30* (2020), 101414
[11] Singh, R., *et al*., Simulated Performance of Packed Bed Solar Energy Storage System Having Storage Material Elements of Large Size – Part I, *The Open Fuels & Energy Science Journal*, *1* (2008), 1, pp. 91-96
[12] Konig-Haagen, A., *et al*., Detailed Exergetic Analysis of a Packed Bed Thermal Energy Storage Unit in Combination with an Organic Rankine Cycle, *Applied Thermal Engineering*, *165* (2020), 114583
[13] Suresh, N. S., *et al*., Modelling and Analysis of Solar Thermal and Biomass Hybrid Power Plants, *Applied Thermal Engineering*, *160* (2019), 114121
[14] Baral, S., Thermodynamic and Financial Assessment of Concentrated Solar Power Plant Hybridized with Biomass-Based Organic Rankine Cycle, Thermal Energy Storage, Hot Springs and CO_2 Capture Systems, *International Journal of Low-Carbon Technologies*, *16* (2021), 2, pp. 361-375

[15] Elouali, A., *et al*., Physical Models for Packed Bed: Sensible Heat Storage Systems, *Journal of Energy Storage*, *23* (2019), June, pp. 69-78
[16] Zanganeh, G., *et al*., Design of Packed Bed Thermal Energy Storage Systems for High-Temperature Industrial Process Heat, *Applied Energy*, *137* (2015), Jan., pp. 812-822
[17] Suresh, C., Saini, R. P., Review on Solar Thermal Energy Storage Technologies and Their Geometrical Configurations, *International Journal of Energy Research*, *44* (2020), Jan., pp. 4163-4195
[18] Lundgaard, C., *et al.*, Density-Based Topology Optimization Methodology for Thermal Energy Storage Systems, *Structural Multidisciplinary Optimization*, *60* (2019), Aug., pp. 2189-2204
[19] Cardenas, B., *et al*., Techno-Economic Optimization of a Packed-Bed for Utility-Scale Energy Storage, *Applied Thermal Engineering*, *153* (2019), May, pp. 206-220
[20] Atalay, H., Cankurtaran, E., Energy, Exergy, Exergoeconomic and Exergo-Environmental Analyses of a Large-Scale Solar Dryer with PCM Energy Storage Medium, *Energy*, *216* (2021), 119221
[21] Lamrani, B., Draoui, A., Thermal Performance and Economic Analysis of an Indirect Solar Dryer of Wood Integrated with Packed-Bed Thermal Energy Storage System: A Case Study of Solar Thermal Applications, *Drying Technology*, *39* (2021), 10, pp. 1371-1388
[22] Eyerer, S., *et al*., Experimental Investigation of Modern ORC Working Fluids R1224yd(Z) and R1233zd(E) as Replacements for R245fa, *Applied Energy*, *240* (2019), Apr., pp. 946-963
[23] Dawo, F., *et al*., R1224yd(Z), R1233zd(E), and R1336mzz(Z) as Replacements for R245fa: Experimental Performance, Interaction with Lubricants and Environmental Impact, *Applied Energy*, *288* (2021), 116661
[24] Huang, J., *et al*., Exergy Analyses and Optimization of a Single Flash Geothermal Power Plant Combined with a Trans-Critical CO_2 Cycle Using Genetic Algorithm and Nelder-Mead Simplex Method, *Geothermal Energy*, *11* (2023), 4
[25] Khalid, F., *et al*., Thermoeconomic Analysis of a Solar-Biomass Integrated Multigeneration System for a Community, *Applied Thermal Engineering*, *120* (2017), June, pp. 645-653
[26] Colantoni, A., *et al*., Performance Analysis of a Small-Scale ORC Trigeneration System Powered by the Combustion of Olive Pomace, *Energies*, *12* (2019), 12, 2279
[27] Mellalou, A., *et al*., Impact of the Greenhouse Drying Modes of Two-Phase Olive Pomace on the Energy, Exergy, Economic and Environmental (4E) Performance Indicators, *Renewable Energy*, *210* (2023), July, pp. 229-250
[28] Gurlek, G., Timurtas, O., Comparative Assessment of Solar Dryer with Thermal Energy Storage System and Heat Pump Dryer in Terms of Performance Parameters and Food Analysis, *Journal of Agricultural Sciences*, *30* (2024), 3, pp. 594-605
[29] Bahrehmand, D., *et al.*, Energy and Exergy Analysis of Different Solar Air Collector Systems with Forced Convection, *Renewable Energy*, *83* (2015), Nov., pp. 1119-1130
[30] Calli, O., *et al*., Energy, Exergy and Thermoeconomic Analyses of Biomass and Solar Powered Organic Rankine cycles, *International Journal of Exergy*, *29* (2019), 2-4, pp. 172-192
[31] Faizan, A., Han, D., Thermophysical Property and Heat Transfer Analysis of R245fa/Al_2O_3 Nanorefrigerant, *The International Journal of Engineering and Science (IJES)*, *5* (2016), 4, pp. 45-53
[32] Aryanfar, Y., *et al.*, Energy, Exergy and Economic Analysis of Combined solar ORC-VCC Power Plant, *International Journal of Low-Carbon Technologies*, *17* (2022), Jan., pp. 196-205
[33] Dupont, C., *et al*., Heat Capacity Measurements Of Various Biomass Types and Pyrolysis Residues, *Fuel*, *115* (2014), 7-8, Jan., pp. 644-651
[34] Mawire, A., *et al*., Simulated Performance of Storage Materials for Pebble Bed Thermal Energy Storage (TES) Systems, *Applied Energy*, *86* (2009), 7-8, pp. 1246-1252
[35] Popovic, M., Thermodynamic Properties of Microorganisms: Determination and Analysis of Enthalpy, Entropy, and Gibbs Free Energy of Biomass, Cells and Colonies of 32 Microorganism Species, *Heliyon*, *5* (2019), 6, e01950
[36] Balli, O., Caliskan, H., On-Design and off-Design Operation Performance Assessments of an Aero Turboprop Engine Used on Unmanned Aerial Vehicles (UAV) in Terms of Aviation, Thermodynamic, Environmental and Sustainability Perspectives, *Energy Conversion and Management*, *243* (2021), 114403
[37] Dhivagar, R., *et al*., Energy, Exergy, Economic and Enviro-Economic (4E) Analysis of Gravel Coarse Aggregate Sensible Heat Storage-Assisted Single-Slope Solar Still, *Journal of Thermal Analysis and Calorimetry*, *145* (2021), pp. 475-449
[38] Tosatto, A., *et al*., Simulation-Based Performance Evaluation of Large-Scale Thermal Energy Storage Coupled with Heat Pump in District Heating Systems, *Journal of Energy Storage*, *61* (2023), 106721
[39] Schwarzmayr, P., *et al*., Exergy Efficiency and Thermocline Degradation of a Packed Bed Thermal Energy Storage in Partial Cycle Operation: An Experimental Study, *Applied Energy*, *360* (2024), 122895

[40] Kedida, D. K., *et al*., Performance of a Pebble Bed Thermal Storage Integrated with Concentrating Parabolic Solar Collector For Cooking, *Journal of Renewable Energy*, *2019* (2019), ID4238549
[41] Turkakar, G., Performance Analysis and Optimal Charging Time Investigation of Solar Air Heater with Packed Bed Sensible Heat Storage Device, *Solar Energy*, *224* (2021), Aug., pp. 718-729

Paper submitted: March 27, 2025
Paper revised: June 25, 2025
Paper accepted: July 29, 2025